PCCP

Accepted Manuscript

This is an *Accepted Manuscript*, which has been through the Royal Society of Chemistry peer review process and has been accepted for publication.

Accepted Manuscripts are published online shortly after acceptance, before technical editing, formatting and proof reading. Using this free service, authors can make their results available to the community, in citable form, before we publish the edited article. We will replace this *Accepted Manuscript* with the edited and formatted *Advance Article* as soon as it is available.

You can find more information about *Accepted Manuscripts* in the **Information for Authors**.

Please note that technical editing may introduce minor changes to the text and/or graphics, which may alter content. The journal's standard **Terms & Conditions** and the **Ethical guidelines** still apply. In no event shall the Royal Society of Chemistry be held responsible for any errors or omissions in this *Accepted Manuscript* or any consequences arising from the use of any information it contains.

Trapping RNase A on MCM41 Pores: Effects on Structure Stability, Product Inhibition and Overall Enzymatic Activity

Irina Matlahov, Yasmin Geiger and Gil Goobes*

Department of Chemistry, Bar Ilan University, Ramat Gan 52900, Israel

ABSTRACT

Catalytic activity of enzymes can be drastically modified by immobilization to surfaces of different materials. It is particularly effective when the dimensions of the biomolecules and adsorption sites on the material surfaces are commensurate. This can be utilized to hinder the biological activity of degradation enzymes and switch of undesired biological processes. Ribonucleases are particularly attractive targets for complete sequestration being efficient at disintegrating viable RNA molecules. Here we show that efficient quenching of ribonuclease A activity can be achieved by immobilization on the surface of MCM41 porous silica. Electron microscopy, isothermal titration calorimetry, differential scanning calorimetry and adsorption

isotherm measurements of ribonuclease A on MCM41 surface are used to demonstrate that the enzyme adsorbs on the external surface of the porous silica through electrostatic interactions that overcome the unfavorable entropy change as the protein gets trapped on the surface, and that immobilization shifts up its denaturtion temperature by 20-25ºC. Real-time kinetic measurements, using single injection titration calorimetry, demonstrate that enzymatic activity towards hydrolysis of cyclic nucleotides is lowered by nearly two orders of magnitude on MCM41 and that active inhibition by the formed product is much less effective on the surface than in solution.

INTRODUCTION

Enzymes immobilized on solid surfaces can undergo anything from stabilization of the native structure by restriction of motions to complete unfolding. At the same time, the catalytic activity of enzymes can be enhanced or completely quenched by immobilization. Lately, it was shown that nanomaterials with surface dimensions matching biomolecule dimensions can prove particularly effective in modifying enzyme structure and activity [1]. Surface curvatures in nanoparticles and in the cavities of porous materials have recently been shown to influence the affinity, surface coverage and structural stability of enzymes [2-3]. Studies monitoring protein conformation on nanoparticle with tunable surface curvature have shown anything from subtle tertiary structural changes to extensive unfolding [4-14]. Improved conformational stability against denaturation on highly curved surfaces was reported for some proteins [9, 11, 15-17], while lower stability was reported for others [18,19]. Enzymatic activity was also shown to be

influenced by surface topology. Catalytic performance of enzymes immobilized on curved surfaces can be either tuned down or enhanced by proper selection of particle size or pore dimensions [4-7,14].

Ribonucleases which play an important role in active RNA degradation in the body are well-studied enzymes. Some members of the ribonuclease family were shown recently to possess cytotoxic activity leading to their utilization in new cancer drugs [20]. Ribonuclease A (RNase A), like its cytotoxic homologue, cleaves RNA molecules specifically after pyrimidine nucleotides. Cleavage takes place in two steps; the second step, in which a cyclic phosphodiester is hydrolyzed to form a 3'-monophosphate, is relatively slow and allows for a complete catalytic characterization [21-22]. The catalytic activity of RNase A in this reaction is known to be competitively inhibited by the product. The binding pocket common to both substrate and product is more often populated by the product generating an active regulation over RNase A's activity.

Efficient sequestration of RNA degradation by the enzyme can be achieved by slowing down this rate determining step which involves cyclic phosphate ring opening. The potential application of designing surfaces that can quench the activity of the enzyme was realized before [23] for numerous industrial and biomedical applications which require RNase – free environment to preserve RNA molecular integrity. A previous study has shown that the catalytic activity of RNase A can be efficiently quenched by immobilization on polyvinylsulfonate coated surfaces [23]. Employing MCM41 with its relatively corrugated outer surface as adsorbent [24], may be advantageous as a stable sustainable inhibitor of RNase A.

The adsorption of RNase A to silica nanoparticles at moderate pH (4-9) is governed by electrostatic interactions that reduce its conformational stability at low salt concentrations [25-27]. Denaturation of the protein on silica particles by heating beyond the melting temperature is partially reversed upon cooling but is thought to be irreversible on porous silica [28]. Recently, it was shown that RNase A molecules penetrate and reside inside cavities in MCM48 mesoporous silica rendering them enhanced structural stability [2]. For MCM41 with hexagonally ordered narrow pores, diffusion into the voids is not expected [2,28]. Activity of the enzyme on silica surfaces shows some interesting behavior as well. On the ordered silica surface of mica, RNase A suffers activity loss initially that is recovered within several hours by reorientation of enzyme molecules on the surface. On silica nanoparticles the enzyme undergoes partial unfolding with minor decrease of its activity [17]. For MCM41 with surface attached dodecyl hydrocarbons, activity is expected to surpass that in solution [28]. To this end, the effect of immobilization of RNase A on mesoporous silica in terms of its catalytic behavior was not reported. Moreover, analysis of catalysis in real-time, to correlate any structural changes in the protein with its ability to bind either the substrate or the product, was not performed.

Using electron microscopy, surface composition analysis and adsorption studies we demonstrate that RNase A is immobilized predominantly on the outer surface of MCM41 [29]. A favorable binding of RNase A to MCM41 surface is observed due to strong electrostatic interactions with the negatively charged silica surface despite the entropy loss observed as the enzyme adsorbs. Differential scanning calorimetry experiments show that RNase A adsorbed on MCM41 undergoes melting at temperatures that are 18°C and 25°C higher than the free molecule reflecting a high conformational stability on the silica surface that is similar to SBA15- or MCM48-entrapped RNase A [2, 28].

4

Effects of surface immobilization on the catalytic activity of RNase A are investigated using kinetic ITC experiments. These measurements reveal nearly complete suppression of catalytic activity on the surface and a concomitant reduction of the maximal turnover rate by two orders of magnitude. Analyzing surface immobilization as a form of inhibition shows that the restraining effect of the silica surface is predominantly uncompetitive, with much smaller impact on the Michaelis constants than on the maximal product formation rate. Consequently, any conformational changes taking place upon immobilization on MCM41 predominantly involve regions in the protein that are away from active site. The effect of immobilization on the substrate and product Michaelis constants is large enough, though, to reverse the relative affinity of the substrate cCMP and product 3'-CMP to the enzyme such that product inhibition is markedly decreased. This is manifested in the drastic changes to the Michaelis-Menten plots collected for the free versus adsorbed enzyme. This results shows that some conformational changes must involve the nucleic acid binding pocket to explain the increased tendency of the substrate to form a complex with the enzyme.

RESULTS AND DISCUSSION

Electron microscopy of RNase A immobilized on MCM41

High resolution scanning electron micrographs (HRSEM) were recorded for MCM41 with and without RNase A. The MCM41 silica particles (Fig. 1a) have an average radius of 70 nm and are characterized by a rough surface. Contrast between dark and bright spots indicate inlets into the long cavities which exist in the porous particles. The micrograph of RNase-MCM41 (Fig. 1b) shows particles of similar size with smooth surface covered with a thin layer which masks the

5

superficial spots observed for the bare particles. High resolution transmission electron micrographs of bare MCM41 (Figs. 1c,d) show the hexagonal ordered pore structure characterizing the inner structure of the particles. The cavity periodicity matches the value extracted from BET and XRD measurements (see Fig. 1s in supporting information) with an average pore diameter of 34 Å and specific surface area of 765 m^2/g. Energy-dispersive X-ray analysis reveals sulfur (Table 1s in supporting information) on the surface of the enzyme-bound MCM41 sample from the 4 cysteine residues in RNase A (0.13 weight %). Transmission electron micrographs of MCM41 particles with RNase A adsorbed could not be recorded without interference by enzyme evaporation under the intense electron beam employed [17]. The ζ-potential measurement of MCM41 particles was measured using ZetaSizer Nano giving rise to -19.17 mV and reflecting the negative charge on this silica surface at pH 5.5. Evidence for binding of the positively charged enzyme to the MCM41 surface is given via a decrease of surface voltage in ζ-potential measurement of [Rnase A•MCM41] to -12.73 mV. The change in surface potential affirms that enzyme molecules cover outer surfaces of the silica and do not reside deep inside the voids.
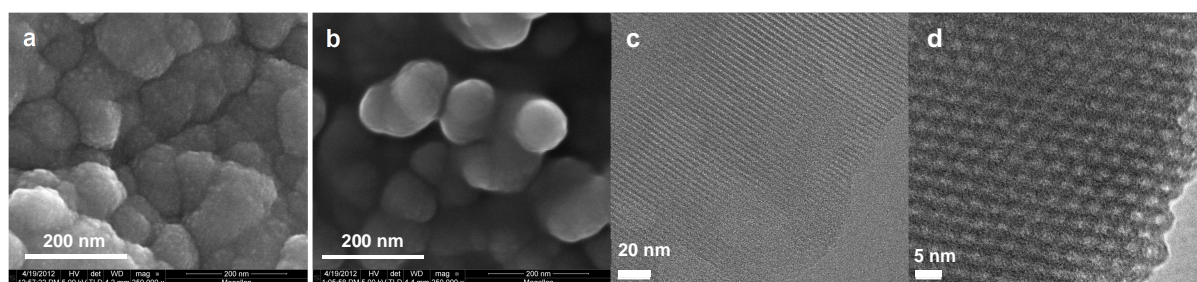

Figure 1. (a) High resolution scanning electron micrographs of MCM41. **(b)** High resolution scanning electron micrographs of RNase A adsorbed on MCM41. **(c)** Transmission electron micrograph providing with a close-up on the particles in (a) and showing their underlying ordered pore structure.

Calorimetric Measurements of RNase A immobilized onto MCM41

Thermodynamic profiling of RNase A binding to MCM41 was performed by ITC measurements. Fig. 2a shows the normalized heat release during titration of 68 µM RNase A into 476 µg/ml suspension of MCM41 in acetate buffer at 30°C, containing 4.52 µM adsorption sites for enzyme molecules. The concentration of adsorption sites is deduced from adsorption isotherm measurements according to the previously suggested procedure [29]. The net heat change with the amount injected into the cell displays a sigmoidal behavior. The adsorption constant K_{ads}, the apparent adsorption enthalpy ΔH_{ads} and the stoichiometry are deduced from fitting the titration curve to a single set of binding sites model which is identical to a simple Langmuir model used to describe adsorption processes [29]. In addition, the apparent adsorption entropy ΔS_{ads} is readily extracted. The values for K_{ads} and ΔG_{ads} extracted are $1.9(\pm 0.3)\times 10^7$ M^{-1} and $-10.0(\pm 0.2)$ kcal·mol^{-1} respectively and the molar ratio is $0.74(\pm 0.02)$. The apparent enthalpic contribution of $-14.5(\pm 0.3)$ kcal·mol^{-1} reflects tight binding driven by electrostatic interactions between RNase A (pI 9.6) and MCM41 surface (point of zero charge 3.2) under current pH conditions. The apparent adsorption entropy ΔS_{ads} is $-14.7(\pm 0.5)$ cal·mol^{-1}·K^{-1} contributing 4.5 kcal·mol^{-1} to the free energy of adsorption. Despite the tendency of RNase A to bind MCM41, immobilization is accompanied by a significant entropic penalty due to restriction of motions when the enzyme adsorbs to the mesoporous material.

In a previous study of RNase A adsorption on silica glass at pH 5.5, a similar Gibbs free energy was measured [30]. The basic residues in the enzyme were suggested as the dominant contributors to the interaction with the negatively charged silica surface and with similar charged surfaces in general [30, 31]. Out of the 4 arginine and 10 lysine residues in RNase A, the

majority are solvent exposed, and amenable to forming electrostatic interactions with the surface groups of MCM41. In other instances where RNase A adsorption is accompanied by unfolding, an entropic gain is observed, associated with increase in motional degrees of freedom in the unfolded state of the protein [32]. Here, the entropy decrease may indicate that the enzyme, considered to be a "hard" protein, retains its structure on the surface and that immobilization attenuates the motions which existed in solution.

Additional thermodynamic measurements of RNase A adsorption to MCM41 surface at low protein concentrations were carried out by adsorption isotherm experiments in order to follow the initial stages of adsorption. The isotherm is plotted in Fig. 2s in the supporting information as the moles of adsorbed RNase A per unit of MCM41 surface area versus the free enzyme concentration (symbols) at 25°C, in acetate buffer. A Langmuir model based fit (solid line) gives rise to a binding constant K_{ads} of $2.0(\pm0.6)\times10^7$ M^{-1} and a maximal surface coverage N_{max} of $0.94(\pm0.05)$ nmol/m^2. The adsorption coefficient is consistent with the value measured in the ITC measurement. The coverage, normalized to the adsorbent surface area, is nearly two orders of magnitude lower than was measured previously on glass silica [30] implying that most of the silica surface of MCM41 is not accessible to the enzyme.
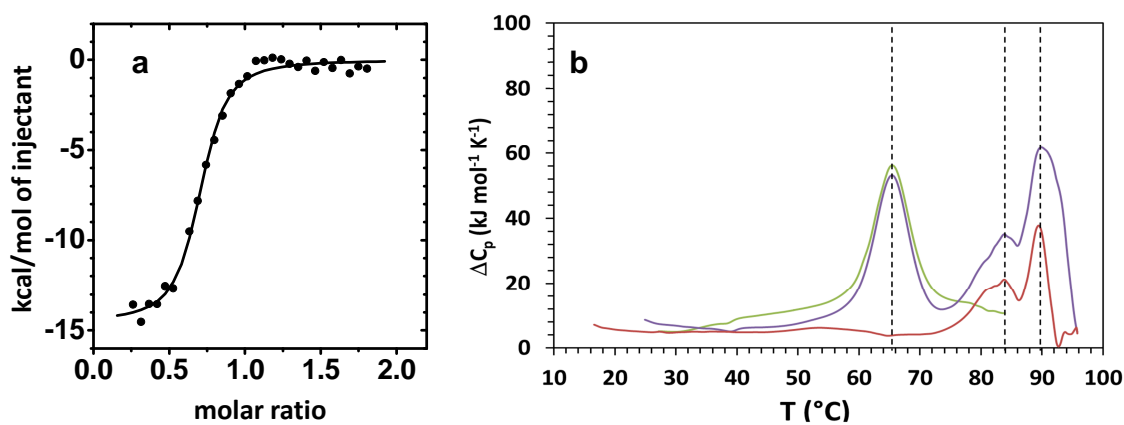
Figure 2. (a) Isothermal titration calorimetry data of 68 μM (0.40 mM in syringe) RNase A adsorbed to 0.476 mg/ml MCM41 suspension (containing 4.52 μM adsorption sites) in acetate buffer (squares) with curve fit based on a single-set of adsorption sites. **(b)** DSC thermograms of 2.2 mg/ml free RNase A in acetate buffer **(green)**, immobilized on 10 mg/ml MCM41 **(red)** and immobilized on 10 mg/ml MCM41 without removal of excess free protein **(purple)**. Contributions from buffer and MCM41 were carefully subtracted out. Dashed lines mark the main observed transitions.

Using total number of RNase A molecules adsorbed at maximal coverage and the footprint of each molecule on the surface (calculated using a hydrodynamic radius of ~1.5-1.7 nm [33-35]), it is found that only 0.8% of the total surface of MCM41 is accommodated. This value is comparable to the percentage of external surface area in MCM41 (1.0-1.5%). Due to geometrical restrictions (similarity between the diameter of the cavities and the dimensions of the enzyme) and the strong electrostatic interactions, entrapment of RNase A inside MCM41 cavities is hindered [28], leading to predominant immobilization of the enzyme to the outer surface of the porous structure. Pore inlets, abundant on external topography of MCM41 owing to the thin pore walls, serve as stable binding sites for trapping RNase A molecules [36, 28].

To evaluate the effect of immobilization on the thermally induced transition from folded to unfolded state, differential scanning calorimetry (DSC) thermograms of free and immobilized RNase A were recorded. These DSC traces are shown in Fig. 2b. For free RNase A (green) thermal denaturation ("melting") is observed at a temperature of $T_m = 65°C$ similarly to previously reported measurements [2, 37]. For RNase A immobilized on 10 mg/ml MCM41 (red), two transitions are observed at $T_m = 84°C$ and $T_m = 90°C$ indicating that immobilized enzyme molecules require higher thermal energy to achieve unfolding as compared to free RNase A. A control thermogram of the enzyme adsorbed to 10 mg/ml MCM41 without removal of excess unbound protein (purple) shows a fraction of free enzyme molecules denaturing at 65°C and the rest adsorbed and denaturing at the two higher temperatures. The higher thermal

energy required for denaturing the immobilized enzyme and resultant increase in melting temperature is associated with the change in configurational energy upon physisorption and the strong electrostatic interactions the enzyme forms with MCM41 [38]. Using statistical thermodynamics model based on random-flight chain description of the unfolded state, it was calculated that the unfolding temperature can increase by more than 10°C, for a protein bound to a wall or a corrugated surface [38]. Adding the protein-surface interactions, can explain the higher shift in the melting temperatures observed.

Previous work describing thermal denaturation of RNase A immobilized on MCM48 surface reported a melting transition at 90°C with a half width of 20°C that was ascribed to enzyme molecules trapped inside the MCM48 pores undergoes [2]. For RNase A immobilized on MCM41 we observe melting transitions with a width at half maximum of 7°C -10°C. The two- to three-fold narrower transitions of the enzyme on MCM41 indicate a narrower distribution of conformational states for the protein on MCM41 [2]. For RNase A chemically tethered to silica beads, denaturation was reported to occur in two subsequent processes at $T_m = 60°C$ and $T_m = 70°C$ associated with unfolding of two separate domains [39, 29]. Here, we observe complete decoupling to two unfolding events with onset of the second melting event after completion of the first melting. These two events may be related to either melting of two separate populations of RNAse A molecules residing in different adsorption sites on the silica surface as seen for binding to MCM48 [2], or alternatively to two subsequent melting processes attributed to two domains in the protein, one which is strongly bound and the other weakly bound to the silica as observed for binding to silica beads [38].

10

Time resolved catalysis performed by both free and immobilized RNase A

Kinetic data is first shown for enzyme molecules partitioned between free and surface immobilized and later for catalysis performed exclusively by surface adsorbed RNase A. The time-resolved catalytic activity of the enzyme is followed by monitoring the time dependent heat change in the sample as cCMP is converted into 3'-CMP using single injection microcalorimetry. The time dependence of the thermal power (dQ/dt), produced during catalytic conversion of cCMP to 3'-CMP at 30 ºC, was recorded using a single 10 μl injection of 20mM cCMP into an ITC cell containing 600 nM of free RNase (cyan) and is shown in Fig. 3a. A typical time-dependent profile of the calorimeter response to the exothermic hydrolysis is shown in the figure. Completion of cCMP hydrolysis is observed after ca. 1500 s as the heat change subsides in accordance with previously observed behavior [19]. The monotonically increasing portion of the curve is used to delineate the reaction kinetics.

Time dependent dQ/dt profiles of cCMP injection (10 μl) into a cell containing 600 nM of RNase A pre-equilibrated with MCM41 concentrations of 238 μg/ml (red), 476 μg/ml (purple) and 952 μg/ml (green) are shown in Fig. 3a. These curves are normalized for convenience to the initial pre-injection power (baseline value) in the free enzyme measurement. A steep decrease in the heat released over time is observed with increase in MCM41 content inside the ITC cell, indicating that catalysis is rapidly quenched as a larger portion of enzyme molecules are immobilized, resulting in fewer cCMP molecules being hydrolyzed per unit of time.

For a quantitative measure of the effect, the reaction velocity, v, and substrate concentration, [S], at each time point are computed from the time dependent dQ/dt values and subsequently Michaelis-Menten plots are constructed (see Fig. 3b) to extract the kinetic

11

parameters. RNase A catalytic activity in ring opening of cCMP molecules, follows a non-standard Michaelis-Menten behavior with concave upwards shape due to inhibitory effect of the product 3'-CMP as noted before [21,22]. It was already shown that the rate equation for product inhibited catalysis can be described by a modified Michaelis-Menten equation:

$$V = \frac{V'_{max}S}{S + K'_m}$$
(1)

with apparent kinetic parameters V'_{max} and K'_m expressed in terms of the original V_{max} and K_m parameters, initial substrate concentration S_0 and product Michaelis constant, K_p as follows:

$$V'_{max} = \frac{K_p V_{max}}{K_p - K_m}, \quad K'_m = \frac{K_m (S_0 + K_p)}{K_p - K_m}$$
(2)

when the condition $0.1 < K_m / K_p < 10$ is fulfilled.

As K_m / K_p becomes much smaller, product inhibition becomes less efficient and the curve shifts from concave upwards, to linear and then to the standard concave downwards curve typical of a simple Michaelis-Menten catalysis [22].
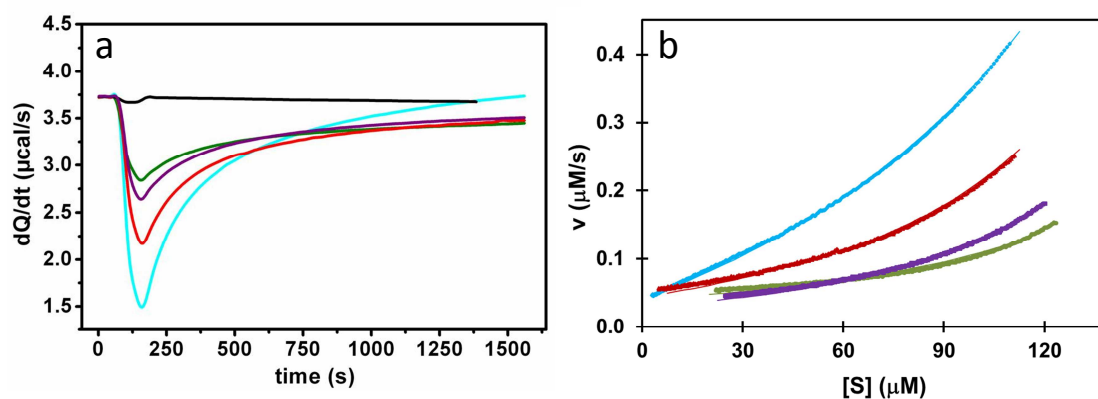
Figure 3. (a) Evolution of the heat signal in the ITC cell after a single injection of cCMP (20 mM) into 600 nM RNase A pre-equilibrated with: 0 (cyan), 238 (red), 476 (purple), 952 (green) µg/ml MCM41. Injection of 20 mM cCMP into 476 µg/ml MCM41 is also shown as a control (black). **(b)** Respective Michaelis-Menten plots extracted from the calorimetry data in (a) using single injection analysis macro by Microcal. Solid lines in (b) represent best fits to measurements using eq 1.

In analysis of experimental data, the apparent kinetic parameters, V'_{max} and K'_m, are deduced using eq 1 and later V_{max} and K_m are extracted from the relations in eqs 2. Analysis of samples comprising free and adsorbed enzyme using eq 1 gives rise to average kinetic parameters representing enzyme molecules in the free and adsorbed states.

The results of fitting the data shown in Fig. 3b are summarized in Table 1. The K'_m value for the enzyme mixed with 238 µg/ml of MCM41 is similar to that of the free enzyme, and at 952 µg/ml MCM41 it increases two-fold in absolute value to -500 µM. The value of V'_{max} on the other hand, decreases in absolute value quite rapidly with increase in MCM41 concentration in the cell to about 6% of its value in free RNase A. By keeping K_p constant, the original kinetic parameters can be extracted readily. These parameters are also reported in Table 1.

A steep decrease in V_{max} is observed as more MCM41 is mixed with the enzyme. This parameter drops to 0.017 µM/s for 952 µg/ml MCM41 reflecting a 64-fold decrease in catalytic activity compared to the free enzyme. Different behavior is observed for K_m which remains practically unchanged at 238 µg/ml MCM41, deceases by 12% at 476 µg/ml MCM41 and by 54% for 952 µg/ml MCM41 (see Table 1). The possibility that adsorbed RNase A is completely inactive and that V_{max} is suppressed by a simple depletion due to adsorption is negated by the observed change in K_m which is expected to stay constant for any concentration of free enzyme.

13

It is worth noting that samples containing MCM41 reach an identical asymptotic value of dQ/dt that is 0.25 µcal/s lower than the pre-injection value (unlike the free enzyme). This heat capacity difference cannot arise from differences in the specific heat capacity of free and adsorbed cCMP since the thermal power produced during single injection of cCMP into MCM41 is negligible (Fig. 3a black line). The heat signal offset can be the result of specific heat capacity difference between free and MCM41-adsorbed 3'-CMP which could contribute directly to the specific heat capacity or indirectly by disparate heat capacities for free and adsorbed [3'-CMP•RNase A] complexes [39].

Table 1. Summary of apparent and original kinetic parameters deduced from fitting the Michaelis-Menten curves in Fig. 3b as a function of MCM41 content.

MCM41 (µg/ml)	V'_{max} (µM/s)	K'_m (µM)	V_{max} (µM/s)	K_m (µM)	K_m/K_p
0	-0.43 (±0.03)	-270 (±15)	1.10 (±0.03)	188 (±11)	3.55
238	-0.11 (±0.01)	-268 (±21)	0.29 (±0.04)	191 (±14)	3.60
476	-0.042 (±0.008)	-294 (±24)	0.082 (±0.01)	155 (±20)	2.92
952	-0.03 (±0.01)	-500 (±47)	0.017 (±0.007)	86 (±10)	1.62

Calorimetry based kinetic measurements of adsorbed RNase A's catalytic activity

Catalytic activity of RNase A immobilized on MCM41 after removal of free and non-specifically adsorbed enzyme molecules was recorded in real-time using the heat response to single injection of substrate. Two samples of 60 µM RNase A immobilized onto 238 µg/ml MCM41 were prepared; one sample where the enzyme and silica adsorbent are allowed to mix, spun down and supernatant is replaced by acetate buffer (sample A) and another sample where

14

the enzyme and silica are allowed to mix and subsequently non-specifically adsorbed enzyme molecules are removed by repeated washes of the RNase A-MCM41 precipitate (sample B). Injections of 20mM cCMP (20 μl) into an ITC cell containing sample A (red) and sample B (blue) are shown in Fig. 4a after conversion into reaction rate versus [S] curves. Data fits using eq 1 are also shown in Fig. 4a and the resultant kinetic parameters are summarized in Table 2. The maximal rates of catalysis by the enzyme in sample A and B are 0.049 μM/s and 0.024 μM/s respectively showing a 22-fold and 45-fold decrease in the maximal rate compared to the free enzyme. The lowest rate of catalysis (sample B) is still ~30 times faster than the non-catalytic hydrolysis rate of cCMP under similar pH and temperature conditions [39].
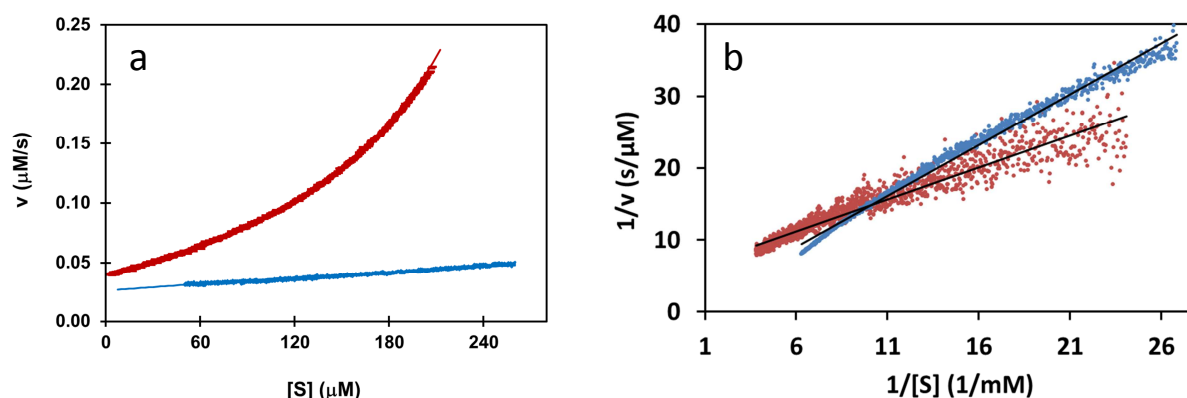

Figure 4. (a) Michaelis-Menten plots derived from single injection data of cCMP (20 mM) into 60 μM RNase A pre-adsorbed to 238 μg/ml MCM41 with free enzyme extracted out, sample A (red) and with non-specific adsorbed enzyme removed, sample B (blue). Solid lines represent best fits using eq 1. **(b)** Lineweaver-Burk representations of the corresponding velocity curves of sample A (red) and sample B (blue) shown in (a).

Sample A and sample B show 2.2-fold and 4.3-fold lower K_m values relative to the free enzyme. The former Michaelis constant still represents an average value of immobilized enzyme and desorbed or non-specifically bound enzyme, weighted by the population of each of these

states. In sample B enzymatic activity is performed strictly by immobilized RNase A. The turnover rate for this sample is slightly higher than for the enzyme immobilized on 952 μg/ml MCM41 due to the 100-fold higher amount of protein initially immobilized leading to a higher amount of enzyme molecules remaining trapped on the surface and performing the catalytic activity. Additional ^{1}H NMR measurements (Fig. 3s in supporting information) confirmed that cCMP does not undergo appreciable hydrolysis on its own simply by adsorption to MCM41.

Kinetics of cCMP hydrolysis catalyzed by immobilized RNase A (Sample B), shows a linear dependence of reaction velocity on substrate concentration and a sign flip in the apparent kinetic parameters which results from a decrease in K_m below K_p (see Table 2). The affinity of the substrate to RNase A on the silica, therefore, becomes higher than that of the product, as opposed to case in solution, and unveils a marked reduction in the ability of 3'-CMP to inhibit enzyme activity. The underlying molecular reasons for this change require further investigation and may be the result of conformational change in the adsorbed enzyme leading to easier substrate binding (under the assumption of constant K_p made here), or alternatively weaker product binding or both effects simultaneously. Similar kinetic measurements of catalysis by the immobilized enzyme only were recorded as a function of temperature between 25°C and 37°C. These measurements, shown in Fig. 4s in the supporting information, show that at room temperature the rate of catalysis is lowest and as the temperature is increased, maximal conversion rate increases with little difference between 30°C and 37°C. Thermal energy, at this temperature range, has negligible effect on the catalytic behavior of the enzyme on MCM41.

The attenuation of activity by immobilization permits a treatment of the surface as a standard inhibitor which can be competitive, uncompetitive or mixed mode. Analyzing the

change in the original kinetic parameters shows an exponential decay of the maximal turnover rate and a linear reduction in K_m indicating a mixed mode inhibition. The more stringent dependence of V_{max} on MCM41 concentration implies that uncompetitive inhibition is predominantly exerted by the surface. Plotting the reaction curves in a reciprocal representation (Fig. 4b) gives another view of the inhibitory effect of adsorption as the change in slope and intercept between two samples can be readily translated into changes in apparent catalytic parameters.

Table 2. Apparent and original kinetic parameters derived from plots in Fig. 4 for free RNase A and immobilized to 238 µg/ml MCM41 with and without free and non-specifically bound enzyme

MCM41 (µg/ml)	$V_{max}^{'}$ (µM/s)	$K_m^{'}$ (µM)	V_{max} (µM/s)	K_m (µM)	E_0 (µM)	K_m/K_p
238	-0.11 (±0.01)	-268 (±21)	0.288(±0.02)	191.0(±14)	0.6	3.60
238 (sample B)	-0.079 (±0.02)	-505 (±76)	0.049 (±0.01)	86.1 (±19)	60	1.62
238 (sample A)	0.15 (±0.03)	1000 (±220)	0.024 (±0.01)	44.4 (±12)	60	0.84

Yoon and Lenhoff [40] have calculated a binding energy of -3.67 kcal/mol for RNase A adsorbed to a negatively charged planar surface with a preferred binding orientation of the active site facing the surface. Electrostatic interactions between basic residues in RNase A and negatively charged groups on MCM41 surface can account for the changes in the catalytic activity. The RNA substrate lies in a deep cleft between two lobes and is cleaved by two catalytic

histidines, His12 and His119. The 2'-3' cyclic phosphate substrate is stabilized by nearby basic residues such as Lys7, Arg33, Lys41 and Lys66. Residues Lys 7, Arg33 and Lys41 lie on the outer surface of RNase A, outside the binding pocket, and can interact with negatively charged groups on MCM41 surface to exert an uncompetitive inhibition effect. The residues involved directly in catalysis, e.g. histidine 12 and 119, lie deep in the binding pocket and may have undergone a more subtle conformation change due to interaction with the silica surface that translates into some form of competitive inhibition.

CONCLUSIONS

Immobilization of RNase A on the pores of MCM41 renders it more stable against thermal denaturation but attenuates its activity towards RNA hydrolysis. Moreover, it shift the balance between substrate and product binding towards the substrate in the course of catalysis leading to lower enzyme sequestration by the product on the surface. Real-time measurements of reaction kinetics for the free and immobilized enzyme in conjunction with DSC, ITC and adsorption isotherm suggest that the inhibition observed in catalytic function of the strongly-bound enzyme molecules is predominantly of uncompetitive nature and that any conformational changes accompanying adsorption occur mostly away from the binding site. This study demonstrates the fundamental effects that enzyme immobilization on a material with cavities of similar dimensions has on its conformation stability and catalytic behavior.

MATERIALS AND METHODS

Materials.   Cytidine 2', 3' – cyclic monophosphate monosodium salt 95-99% (cat. number C9630) and Ribonuclease A (cat. number R5500) from bovine pancreas (Type 12-A, activity ~100 Kunitz units/mg protein $\geq$90%) were purchased from Sigma-Aldrich. MCM41 (cat. number 643645) mesoporous silica was also purchased from Sigma-Aldrich and used as is. This silica material is prepared according to procedure suggested before [42]. Sodium acetate buffer, 50 mM pH 5.5 was used in all experiments carried out in this work. Two samples of RNase A adsorbed to MCM41 with non-specific adsorbed enzyme removed (sample A) and with only the free desorbed enzyme taken out (sample B) were prepared in the following way. Sample A was prepared by repeated washes using acetate buffer and leaving the enzyme-silica complex for 2 hours for equilibration until no enzyme was detected in the supernatant. Sample B was prepared by a single exchange of supernatant solution containing desorbed enzyme by acetate buffer after adsorption was completed. These samples were used immediately after preparation in the DSC and kinetic calorimetry measurements.

Electron Microscopy. High resolution scanning electron microscopy was performed on samples of MCM41 and RNase A-MCM41 in acetate buffer using a Magellan XL400 FEI microscope, with e-beam voltage of 5 kV and operating at high resolution mode. Samples were dried under N_2 flow, deposited on carbon coated grid and then were covered by carbon before micrographs were taken.

ζ Potential measurements. The surface charge of MCM41 and enzyme-bound MCM41 particles in dispersion were measured by a ZetaSizer Nano-ZS (Malvern Instruments Ltd., Worcestershire, UK). Size measurements were performed by the dynamic light scattering (DLS) method of dilute nanoparticle dispersions ($\approx$0.5 mg/mL) in EtOH, i-PrOH, or H2O. The samples were sonicated

for 1−2 min before analysis. The ZetaSizer Nano series was also used for determining the ζ potential of NPs by measuring electrophoretic mobility and then applying the Henry equation.

Adsorption Isotherms. Binding of RNase A to surface of MCM41 was investigated through adsorption isotherm measurements. Different RNase A solutions in sodium acetate buffer (pH=5.5) with concentrations of 2 µg/ml to 40 µg/ml were separately mixed with 2.5 mg/ml suspension of MCM41 and stirred for 1 hour. A total of 3.2 µg RNase A was mixed with 200 µg of MCM41 at saturation. Samples were prepared in triplicates for each protein concentration and isotherm experiments repeated at least 4 times to assure reproducibility. After spin-down and incubation, the protein concentration in the supernatant was determined using a Micro BCA protein assay reagent kit (Pierce) recording the absorbance at 562 nm on a TECAN infinite 200 plate reader. The instrument was calibrated by duplicate measurements of RNase A samples with known variable concentrations. The amounts of bound RNase A were determined by subtraction of the measured free enzyme concentration after adsorption from the initially added concentration.

Differential scanning calorimetry were carried out on a Mettler-Toledo DSC 1 instrument using sealed 30 µl containers run at a scan rate of 1 ºC/s and using acetate buffer as reference for the free enzyme measurement and proper MCM41 concentration in acetate buffer as reference for each RNase A-MCM41 measurements. Enzyme concentration was 2.2 mg/ml in all samples and MCM41 concentration was 10 mg/ml. Prior to measurements the enzyme was allowed to bind to MCM41 for an hour and later either measured immediately (sample A) or rinsed extensively to remove free and non-specifically bound RNase A molecules (sample B).

20

Isothermal Titration Calorimetry (ITC).   All calorimetry experiments were carried out on a

Microcal, GE Healthcare VP-ITC calorimeter using high gain mode. Kinetic parameters of

enzymatic reaction were measured at 30°C with the single injection method. Solutions of 0.6 µM

RNase A in acetate buffer 50 mM pH 5.5 and 20 mM cCMP in the same acetate buffer were

prepared and degassed under vacuum for 10 min. The syringe (294 µL) was filled with the

cCMP solution. The sample cell was filled with RNase A solution with increasing concentration

of MCM41 and stirred at 307 rpm for an hour. Kinetic experiments were performed with the

single injection method, injecting 10 µL of cCMP and recording heat change for 1500 seconds

and at MCM41 concentrations of 0, 238.1 , 476.2, 952.4 µg/ml. The thermal power (dQ/dt) in

watts was recorded every 1 sec. The minima in the dQ/dt curves is observed 90 s post injection

in accordance with the expected response time for a VP-ITC microcalorimeter [19].The data

were fit to kinetic equations using Origin Lab 7 and using previously reported affinity constant

of 3'CMP [21]. To correct for non-zero intercept in the velocity curves (see Figs. 3-4), S is

replaced by $S - S_{offset}$ in eq 1 as suggested before [22]. The S_{offset} parameter is included in fitting

these velocity curves. Calorimetric thermodynamic measurements of RNase A adsorption on the

mesoporous silica at 30 °C were carried out by titrating 200 µl of 0.4 mM RNase A (20

injections of 10 µl each) into a sample cell containing 1.4 ml with MCM41 concentration of

476.2 µg/ml and equilibrated. A total of 0.08 µmol RNase A has been titrated onto a total of 672

µg of MCM41.

ASSOCIATED CONTENT

AUTHOR INFORMATION

Corresponding Author

To whom correspondence should be addressed: *E-mail: gil.goobes@biu.ac.il, Ph: +972-3-531-7390, Fax: +972-3-738-4053.

Notes

The authors declare no competing financial interest.

REFERENCES

1. Natalio, F.; Andre, R.; Hartog, A. F.; Stoll, B.; Jochum, K. P.; Wever, R.; Tremel, W. *Nat. Nanotechnol.* **2012** 7, 530-535; Liao, Y.-J.; Shiang, Y.-C.; Huang, C.-C.; Chang, H.-T. *Langmuir* **2012**, *28*, 8944-8951; Wu, Z.; Zhang, B.; Yan B. *Int. J. Mol. Sci.* **2009**, 10, 4198-4209; Hartmann, M. *Chem. Mater.* **2005**, 17, 4577-4593.

2. Ravindra, R.; Zhao, S.; Gies, H.; Winter, R. *J. Am. Chem. Soc.* **2004** *126*, 12224–12225.

3. Vertegel, A. A.; Siegel, R.W.; Dordick, J. S. *Langmuir* **2004,** *20*, 6800-6807; Lundqvist, M.; Sethson, I.; Jonsson, B. H. *Langmuir* **2004,** *20*, 10639-10647.

4. Luckarift, H. R.; Spain, J. C.; Naik, R. R.; Stone, M. O. *Nature Biotechnology* **2004**, *22*, 211–213.

5. Lei, C. H.; Shin, Y. S.; Liu, J.; Ackerman, E. J. *J. Am. Chem. Soc.* **2002**, *124*, 11242–11243.

6. Xiao Y., Patolsky F., Katz E., Hainfeld J.F., Willner I., *Science* **2003** *299*, 1877-1881.

7. Brockman, H. L.; Law, J. H.; Kezdy, F. J. *J. Biol. Chem.* **1973,** *248*, 4965–4970.

8. Kim, D.; Blanch, H. W.; Radke, C. J. *Langmuir* **2002,** *18*, 5841–5850.

9. Goobes, G.; Goobes, R.; Schueler–Furman, O.; Baker, D.; Stayton, P. S.; Drobny, G. P. *Proc. Natl. Acad. Sci. USA* **2006**, *103*, 16083–16088.

10. Masica, D. L.; Ash, J. T.; Ndao, M.; Drobny, G. P.; Gray, J. J. *Structure* **2010,** *18*, 1678–1687.

11. Masica, D. L.; Gray, J. J.; Shaw, W. J. *J. Phys. Chem. C* **2011**, *115*, 13775–13785.

12. (a) Diaz, J. F.; Balkus, K. J. Jr. *J. Mol. Catal. B: Enzymatic* **1996,** *2*, 115-126. (b) Washmon–Kriel, L.; Jimenez, V. L.; Balkus, K. J. Jr. *J. Mol. Catal. B: Enzymatic* **2000,** *10*, 453-469.

13. (a) Takahashi, H.; Li, B.; Sasaki, T.; Miyazaki, C.; Kajino, T.; Inagaki, S. *Micropor. Mesopor. Mater.* **2001,** *44*, 755-762. (b) Takahashi, H.; Li, B.; Sasaki, T.; Miyazaki, C.; Kajino, T.; Inagaki, S. *Chem. Mater.* **2000,** *12*, 3301-3305.

14. (a) Deere, J.; Magner, E.; Wall, G. J.; Hodnett, B. K. *Catal. Lett.* **2003**, *85*, 19-23. (b) Katiyar, A.; Ji, L.; Smirniotis, P. G.; Pinto, N. G. *Micropor. Mesopor. Mater.* **2005,** *80*, 311–320.

15. Asuri, P.; Karajanagi, S. S.; Yang, H. C.; Yim, T. J.; Kane, R. S.; Dordick, J. S. *Langmuir* **2006**, *22*, 5833-5836.

16. Karajanagi, S. S.; Vertegel, A. A.; Dordick, J. S. *Langmuir* **2004,** *20*, 11594-11599.

17. Shang, W.; Nuffer, J. H.; Dordick, J. S.; Siegel, R. W. *Nano Lett.* **2007**, *7*, 1991–1995.

18. Roach, P.; Farrar, D.; Perry, C. C. *J. Am. Chem. Soc.* **2006**, *128*, 3939-3945.

19. Noinville, S.; Revault, M. Ed. by DéJardin P. **2006,** part II 119–150 "Conformations of Proteins Adsorbed at Liquid-Solid Interfaces" Springer Berlin Heidelberg.

20. Rutkoski, T. J.; Raines, R. T. *Curr. Pharmaceut. Biotech.* **2008,** *9*, 185–199.

21. Spencer, S. D.; Raffa, R. B. *Pharmaceu. Research* **2004**, *21*, 1642–1647.

22. Koerber, S.; Fink, A. *Analytic. Biochem.* **1987**, *165*, 75–87.

23. Smith, B. D.; Soellner, M. B.; Raines, R. T. *Langmuir* **2005,** *21*, 187–190.

24. Kresge, C. T.; Leonowicz, M. E.; Roth, W. J.; Vartuli, J. C.; Beck, J. S. *Nature* **1992**, 359, 710-712.

25. Iwaoka, M.; Sano, N.; Hasegawa, N.; Yokokawa, M.; Kunigami, S.; Shirai, H. *Bull. Chem. Soc. Jpn.* **2010**, *83*, 935–941.

26. Larsericsdotter, H.; Oscarsson, S.; Buijs, J. *J. Colloid. Interf. Sci.* **2001,** *237*, 98–103.

27. Kondo, A.; Higashitani, K. J. *J. Colloid. Interf. Sci.* **1992,** *150*, 344–351.

28. Zhao, S. *Differential Scanning and Pressure Perturbation Calorimetric Studies on Proteins Confined in Mesoporous Molecular Sieves* PhD dissertation, Dortmund University, **February 2007**.

29. Rialdi, G.; Battistel, E. *Proteins* **1994**, *19*, 120-131.

30. Goobes, R.; Goobes, G.; Campbell, C. T.; Stayton, P. S. *Biochemistry* **2006,** *45*, 5576-5586.

31. Hummel, J. P.; Anderson, B. S.; *Arch. Biochem. Biophys.* **1965**, *112*, 443-447.

32. Gerstner, J. A.; Bell, J. A.; Cramer, S. M. *Biophys. Chem.* **1994**, *52*, 97–106.

33. Panick, G.; Winter, R. *Biochemistry* **2000**, *39*, 1862–1869.

34. Sosnick, T. R.; Trewhella, J. *Biochemistry* **1992,** *31*, 8329–8355.

35. Nöppert, A.; Gasta, K.; Müller–Frohne, M.; Zirwer, D.; Damaschun, D. *FEBS Letters* **1996**, *380*, 179–182.

36. Hoffman, F.; Cornelius, M.; Morell, J.; Froba, M. *Angew. Chem. Int. Ed.* **2006**, *45*, 3216–3251.

37. Gharanfoli, M.; Moosavi-Movahedi A. A.; Safarian, S.; Chamani, J.; Saboury, A. A. *Thermochim. Acta* **2004,** *411*, 37-42.

38. Battistel, E.; Sabbioneta, P.; Rialdi, G. *Thermochim. Acta* **1990,** *172*, 21–30; Battistel, E.; Bianchi, D.; Rialdi, G. Pure Appl. Chem. **1991**, *63*, 1483-1490.

39. Eftink, M. R.; Biltonen, R. L. *Biochemistry* **1983,** *22*, 5134-5140.

40. Yoon, B. J.; Lenhoff A. M. *J. Phys. Chem.* **1992**, *96*, 3130-3134.

41. Zhou, H.-X.; Dill, K. A. *Biochemistry* **2001**, *40*, 11289-11293.

42. Beck, J. S.; Vartuli, J. C.; Roth, W. J.; Leonowicz, M. E.; Kresge, C. T.; Schmitt, K. D.; Chu,

C. T. W.; Olson, D. H.; Sheppard, E. W.; McCullen, S. B.; Higgins, J. B.; Schlenker, J. L. *J. Am.*

Chem. Soc. **1992**, *114*, 10834-10854.

Graphical Table of Content
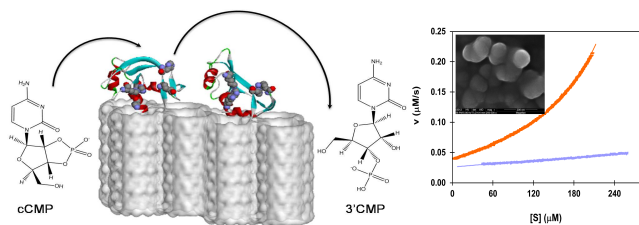
Ribonuclease's Activity bound to nano-sized pore openings of MCM41 is severely quenched but inhibition by the product is reduced